International Journal of Thermofluids 3–4 (2020) 100030

Contents lists available at ScienceDirect

International Journal of Thermofluids

journal homepage: www.elsevier.com/locate/ijtf

Current density and criticality branch-chain for a reactive Poiseuille second-grade hydromagnetic flow with variable electrical conductivity

S.O. Salawu*[,a], E.O. Fatunmbi[b]

[a] Department of Mathematics, Landmark University, Omu-Aran, Nigeria
[b] Department of Mathematics and Statistics, Federal Polytechnic, Ilaro, Nigeria

ARTICLE INFO

Article History:
Received 28 January 2020
Revised 30 March 2020
Accepted 30 March 2020
Available online 21 April 2020

Keywords:
Electrical conductivity
Poiseuille flow
Current density
Thermal criticality
Chemical kinetic

ABSTRACT

This study investigates the current density and branch-chain thermal criticality for a non-Newtonian hydromagnetic second-grade fluid flow in a Poiseuille device with varying electrical conductivity. The combustible reactive fluid is fully exothermic without material consumption, and the fluid is induced by electric and magnetic fields in the presence of axial gradient pressure. With suitable variables, the equations are translated to dimensionless form and solved by semi finite discretization difference scheme to provide solutions for the heat and velocity dependent parameters. The thermal ignition and slice bifurcation for the criticality, and the current density results are plotted for various dependent terms. It is obtained from the investigation that terms that increases current density in the flow system need to be augmented to improve the current carrying hydromagnetic fluid in order to improve its industrial usage.

1. Introduction

In dynamical flow system, laminar flow of an.incompressible fluid in space within a parallel fixed wall described Poiseuille flow. A flow in which pressure drop in necessary to set the fluid in motion. Poiseuille flow is significant in determining the vascular resistance and hence flow rate of intravenous fluids that may be achieved using various sizes of peripheral and central cannulas, the flow is applicable in medical science, engineering and industrial processes [1–3]. However, several liquids used in technology and manufacturing systems such as drilling mud, polymer solutions, coal slurries, grease, hydrocarbon oils and so on are chemically reactive. These reactive substances are exposed to extreme circumstances during processes, like high shear rate, pressure and temperature [4–7]. In fact, coupling with different kinetics and shear rates, friction between the walls and the liquid generates high heat that impacts the lubricants viscosity and other fluids property [8,9]. Moving the liquid into a cooling reservoir or by using an additives will assist is improving the fluid characteristics, Kobo and Makinde [10] Non-Newtonian fluids can serve as an additives most especially non-Newtonian viscoelastic fluid among which is second-grade fluid with simple rheological properties, Salawu et al. [11,12]. The fluid is the simplest differential type of viscoelastic subclass liquid with applications in modern industries and technology.

Due to the uses of second-grade fluid, semi-analytical techniques for unsteady second-grade liquid over a moving plate was examined by [13–15]. The significance of different terms on the momentum modules was reported in the study. Flow fluid and energy transport phenomena in a channel have a significant usefulness in industrial processes such as production of paper, wire drawing, film sheet and many more, Kareem et al. [16]. In the presence of heat transfer, but without exothermic reaction, Hayat et al. [17,18] considered the effect of some pertinent terms on the steady state of second-grade hydromagnetic viscous dissipative fluid. The problem was reduced to dimensionless form using transformation variables and solved by Homotopy analysis method. The unsteady state of heat transfer second-grade magnetohydromagnetic fluid has been reported without considering reactive chemical species and induced electric field, among are [19–22]. Nevertheless, time to time changes in temperature momentously impacted the effectiveness of most reactive species used in engineering processes. A rise in the heat generated in a reactive system can lead to thermal blowup of the system.

Thermal stability study of the critical state performs an important role in processing and handling of viscoelastic second-grade fluid. Critical state occurs when the diffusion of heat to the environment in a reactive system is lesser than the heat produced [23,24]. Therefore, it is necessary to determine the thermal criticality conditions for the effective uses of second-grade fluid. This condition connotes thermal runaway or explosion that can assist in the prediction of unsafe or safe state of reactive flow conditions. In view of these, Makinde [25,26] examined thermal criticality of a reactive flow in a channel with viscous dissipation using an approximation technique. The

* Corresponding author.
E-mail address: salawu.sulyman@lmu.edu.ng (S.O. Salawu).

https://doi.org/10.1016/j.ijft.2020.100030

bifurcation slice plot for Nusselt number against Frank-Kamenetskii is presented for non-Newtonian material term and activation energy. The diagram shows reactive system criticality or ignition. Okoya [24,27] reported on the criticality and the disappearance of criticality for a flow of reactive exothermic chemical combustion is a channel. The maximum heat criticality and Frank-Kamenetskii criticality are obtained for the fluid flow. All these studies were done without time variation, induced electric field, variable conductivity.

Follow from Chinyoka and Makinde [28], this study examines the current density and branch-chain criticality for a reactive second-grade fluid. It is imperative to study the effect of temperature dependent electrical conductivity for current density in order to improve the current carrying hydromagnetic fluid for industrial usage. This is necessary in order to enhance lubricants viscosity for the operations of manufacturing and engineering device at optimum performance. The combustible reactive fluid is assumed to take place in a Poiseuille device with non-uniform wall temperature. This study has not been previously examined in its present form. The study overview is as follows: mathematical setup is given in section two, while numerical analysis and application is demonstrated in section three. Section four contains the results and discussion which then follow by conclusion from the study.

2. Mathematical formulation

The transient combustible hydromagnetic second-grade reactive fluid flow in a Poiseuille device is examined in the existence of induced electric field $\mathbf{E_f}$, imposed magnetic field $\mathbf{B_0}$, and temperature reliance conductivity $\sigma(T)$. As displayed in Fig. 1, the flow is along horizontally fixed device with unequal wall temperature.

The dynamically Cauchy tensor formulation for the second-grade that is kinematical related is expressed as Fosdick and Rajagopal [29],

$$\mathbf{T} = -p\mathbf{I} + \mu\mathbf{B_1} + \phi_1\mathbf{B_2} + \phi_2\mathbf{B_1^2}, \tag{1}$$

The terms p denotes pressure, $\mathbf{I}$ represents tensor identity, μ connotes viscosity, ϕ_1 and ϕ_2 illustrate the material, and $\mathbf{B_1}$ and $\mathbf{B_2}$ are the tensors kinematical (see Ali et al. [22]) which are defined as follows

$$\mathbf{B_1} = \nabla\mathbf{W} + (\nabla\mathbf{W})^{T_r}, \quad \mathbf{B_2} = \frac{d\mathbf{B_1}}{dt} + \mathbf{B_1}(\nabla\mathbf{W}) + (\nabla\mathbf{W})^{T_r}\mathbf{B_1}, \tag{2}$$

here, T_r is the transpose, d/dt is the derivative of the material, $\mathbf{W}$ is the velocity of the fluid, and the dynamically satisfied moduli material constraints are given as Sajid et al. [20]

$$\mu \geq 0, \quad \phi_1 \geq 0, \quad \phi_1 + \phi_2 = 0. \tag{3}$$

For the active species, the single velocity fluid balance according to Truesdell [30] is expressed as

$$\rho\frac{d\mathbf{W}}{dt} = div\mathbf{T} - \mathbf{J}\times\mathbf{B} + \rho\mathbf{f}, \tag{4}$$

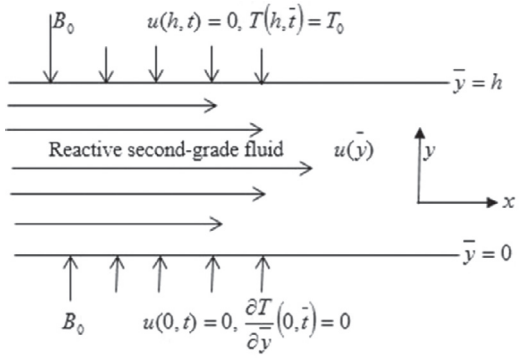

Fig. 1. The Geometry of the flow

where $\mathbf{f}$ denotes the body force, $\mathbf{J}\times\mathbf{B}$ corresponds to the Lorentz force (MHD), with $\mathbf{B}$ being the magnetic field and $\mathbf{J}$ stands for the current density. The current density is taken from Ohm's law with variable conductivity as Salawu et al. [23]

$$\mathbf{J} = \sigma(T)(\mathbf{E_f} + \mathbf{W}\times\mathbf{B}), \tag{5}$$

where $\mathbf{E_f}$ is the electric field, $\mathbf{B} = \mathbf{b} + \mathbf{B_0}$ and $\mathbf{b}$ is the induced magnetic field. The electrical heat dependent conductivity $\sigma(T)$ is defined as [23,31]

$$\sigma(T) = \sigma_0\left[\frac{E(T-T_0)}{T_0^2R}\right]^m, \tag{6}$$

where the term m is the heat index and σ_0 denote the conductivity. The exothermic second-grade combustible reaction energy balance is taken as

$$\rho\frac{d\chi}{dt} = \rho r - div\mathbf{q} + \mathbf{T}\cdot\mathbf{L} + QCA, \tag{7}$$

where r is the heat radiant, $\mathbf{q}$ is the vector heat flux, χ is the internal energy specific, $\mathbf{L}$ is the gradient velocity, C is the reactant initial species, Q is the reaction heat and A is the temperature dependent reaction rate. The branch chain term A with activation energy E is assumed to be a general rate law of reaction written as Okoya [27]

$$A = A_0\left(\frac{kT}{\nu l}\right)^n exp\left(-\frac{E}{RT}\right), \tag{8}$$

for the process examined here, the consumption reactant is ignored because it is very small with no significant effect. The parameter A_0 is the constant branch chain rate order, n is the pre-index factor taking from Bimolecular kinetics, ν is the vibration frequency, k is the Boltzmann constant, R is the constant universal gas, l is the Planck's number and T is the temperature.

Follow from the above assumptions, the approximations dimensionless boundary layer for the hydromagnetic second-grade reactive momentum and heat equations with variable conductivity are taken after [22,28] as follows:

$$\frac{\partial w}{\partial t} = \frac{\partial^2 w}{\partial y^2} + \Lambda\frac{\partial^3 w}{\partial y^2\partial t} + G - M(\delta + w)\theta^m, \tag{9}$$

$$Pr\frac{\partial\theta}{\partial t} = \frac{\partial^2\theta}{\partial y^2} + Br\left[\Lambda\frac{\partial w}{\partial y}\frac{\partial^2 w}{\partial y\partial t} + \left(\frac{\partial w}{\partial y}\right)^2 + M(\delta + w)^2\theta^m\right] + \lambda(1 + \epsilon\theta)^n exp\left(\frac{\theta}{1+\epsilon\theta}\right), \tag{10}$$

With the suitable non-dimensional boundary and initial conditions

$$w(y,0) = 0, \quad \theta(y,0) = \theta_r, \quad w(0,t) = 0, \quad \frac{\partial\theta}{\partial y}(0,t) = 0, \quad w(1,t) = 0, \quad \theta(1,t) = 0. \tag{11}$$

The consequential variables of Eq. (12) are used to obtain the Eqs. (9)–(11).

$$\theta = \frac{E(T-T_0)}{RT_0^2}, \lambda = \frac{EA_0CQh^2}{RT_0^2k_0}\left(\frac{kT_0}{\nu l}\right)^n e^{-\frac{1}{\epsilon}}, \theta_a = \frac{E(T_a-T_0)}{RT_0^2}, \epsilon = \frac{RT_0}{E}, M = \frac{\sigma_0 h^2B^2}{\mu},$$
$$P = \frac{h\bar{P}}{\mu U}, G = -\frac{\partial P}{\partial x}, Pr = \frac{\mu Cp}{k_0}, Br = \frac{EU^2\mu}{RT_0^2k_0}, w = \frac{\bar{u}}{U}, t = \frac{\bar{t}\mu}{\rho h^2}, \Lambda = \frac{\alpha_1}{\rho h^2}, \delta = \frac{E_f}{UB}, y = \frac{\bar{y}}{h}. \tag{12}$$

where the terms λ, ϵ, Λ, M, w, θ_a, G, Pr, θ, Br and δ are the Frank-Kamenetskii, activation energy, second-grade Material, Magnetic, Velocity, initial temperature, pressure gradient, Prandtl number, fluid temperature, Brinkman number, loading electric field. The current density and total current produced in the considered reactive hydromagnetic exothermic combustible system is given as Salawu et al. [31]. Current density measures the quantity of charges that flow

through a chosen sectional area per unit time.

$$\begin{aligned} J &= (w+\delta)\theta^m \qquad \text{(Current density)} \\ Ip &= \int_0^1 (w+\delta)\theta^m dy \qquad \text{(Total produced current)} \end{aligned} \tag{13}$$

It is very necessary to be aware that, for a configuration of short electric circuit in which loading electric field is not present, then $\delta = 0$.

Limiting cases

Note that when $\Lambda = \lambda = 0$, this study corresponds to the one done by Chinyoka and Makinde [28] with no report on the current density. When $\delta = 0$ with constant viscosity for a second-grade fluid, the study is equivalent to Rundora and Makinde [32] with $\gamma = s = Bi = 0$ and Makinde and Chinyoka [33] with $\gamma = Bi = 0$. When $\delta = \lambda = Br = 0$, the work is related to that of [19,21,22].

3. Numerical analysis

The finite semi-discretization difference method presented by Chiyoka [34] is employed. As used in Salawu et al. [7], the method is assumed with time level intermediate $z + \varphi$ where $\varphi \in [0, 1]$. The linear uniform grid and Cartesian mesh are the basis for the model equations on which finite difference discretization is defined. Central difference of second order is taken for the approximation of the spatial derivatives. The boundary conditions are incorporated into the equations by modifying the grid last and first points. The discretization module for the velocity balance is illustrated as

$$\frac{\partial}{\partial t}\left(w - \Lambda\frac{\partial^2 w}{\partial y^2}\right) = -M(\delta + w^{z+\varphi})(\theta^m)^z + G + \frac{\partial^2}{\partial y^2}w^{z+\varphi}, \tag{14}$$

Then w^{z+1} gives

$$-f_1 w_{j-1}^{z+1} + f_2 w_{j-1}^{z+1} - f_1 w_{j+1}^{z+1} = -\Delta t M(1-\varphi)(\delta + w^z)(\theta^m)^z + (w + \Lambda w_{yy})^z + \Delta t G + \Delta t(1-\varphi)w_{yy}^z, \tag{15}$$

where $f_1 = \frac{1}{\Delta y^2}(\Lambda + \varphi\Delta t)$, $f_2 = (1 + \varphi\Delta t M + 2f_1)$. The solving algorithm for the w^{z+1} becomes a matrices of tri-diagonal inversion, which serves as a merit over complete implicit method. The integration techniques of the semi-discretization of partial differentiation for the temperature balance module becomes

$$Pr\frac{\theta^{z+1} - \theta^z}{\Delta t} = Br\left[\Lambda\frac{\partial w}{\partial y}\frac{\partial^2 w}{\partial y \partial t} + \left(\frac{\partial w}{\partial y}\right)^2 + M(\delta + w)^2\theta^m\right]^z + \frac{\partial^2}{\partial y^2}\theta^{z+\varphi} + \lambda\left[(1+\epsilon\theta)^n e^{\left(\frac{\theta}{1+\epsilon\theta}\right)}\right]^z, \tag{16}$$

Then θ^{z+1} gives

$$f\theta_{j-1}^{z+1} + (Pr + 2f)\theta_j^{z+1} - f\theta_{j+1}^{z+1} = \theta^z + \lambda\Delta t\left[(1+\epsilon\theta)^n e^{\left(\frac{\theta}{1+\epsilon\theta}\right)}\right]^z + \Delta t(1-\varphi)\theta_{yy}^z + Br\left[\Lambda\frac{\partial w}{\partial y}\frac{\partial^2 w}{\partial y\partial t} + \left(\frac{\partial w}{\partial y}\right)^2 + M(\delta + w)^2\theta^m\right]^z, \tag{17}$$

where $f = \frac{\varphi\Delta t}{\Delta y^2}$. The algorithm for θ^{z+1} in the solution gives inverse matrices in tri-diagonal form. The techniques in Eqs. (15) and (17) are tested in time and space for accuracy when $\varphi = 1$ as well as the consistence. Here, $\varphi = 1$ is chosen to enable large steps of time until a solutions steady convergence is obtained.

4. Results and discussion

The transient solutions for the heat and momentum profiles are obtained using a finite semi-discretization difference method. The used parameters values are based on the existing related works done, and the initial reactive combustible temperature θ_r is assumed to be equal to the temperature at the wall. With finer mesh ($\Delta y = 0.001, \Delta t = 0.01$), the transient three dimensional solutions are shown in Figs. 2 and 3. A transient rise till a steady state is achieved in the flow rate and energy fields are observed.

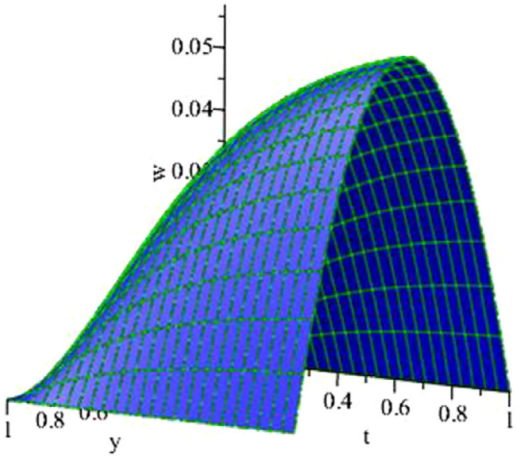

Fig. 2. 3D Flow field for time variation.

4.1. Velocity and temperature parameters solutions dependent

The plot of $w(y, t)$ against y for different values of the dependent parameters Λ and δ on the electrically conducting second-grade fluid is displayed in Figs. 4 and 5. Both terms oppose the flow rate as seen in the plots. The second-grade material term Λ in Fig. 4 enhances the viscoelastic bonding force that in turn drags the velocity profile. Also, the electric loading field δ exerts force due to Lorentz force radially opposite the moving fluid that leads to declination in the flow velocity profile. An increase in the values of both terms boosted the viscoelastic property of the fluid. Therefore, using the material as a lubricant, both terms should be enhanced for effective performance of an industrial machine. The response of the exothermic heat transfer to rising in the values of electric field loading δ and Brinkman number Br is demonstrated in Figs. 6 and 7. Both parameters encourage the temperature distribution magnitude in the device by increasing the reactive combustion internal heat production in the system. Therefore, the combustion process rate is boosted as the reaction activation energy enhances the exothermic reaction in the presence of bimolecular kinetics. Hence, the temperature distribution in the conducting liquid is enhanced as the value of the terms increases.

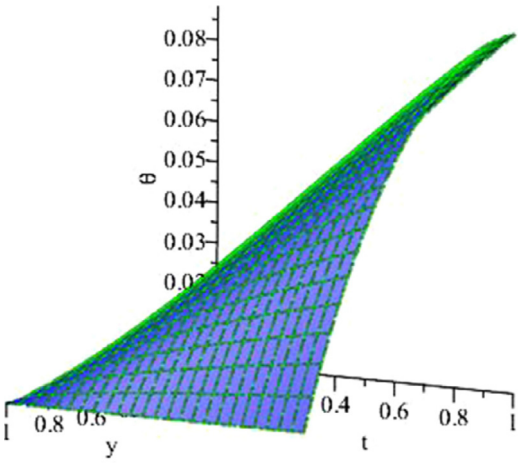

Fig. 3. 3D heat profile for time different.

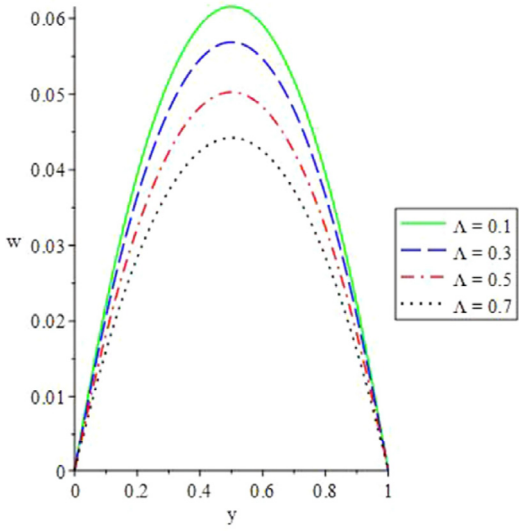

Fig. 4. Velocity field for increasing Λ.

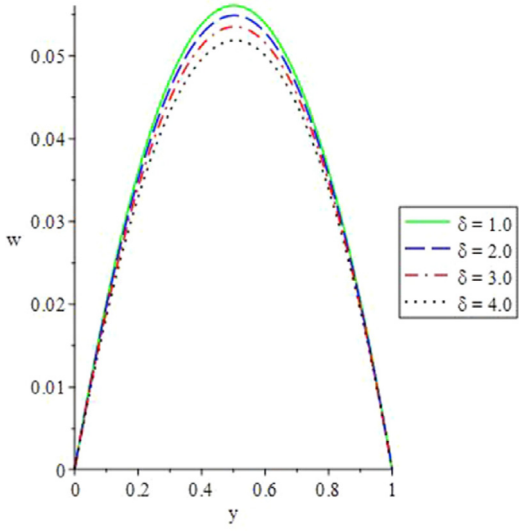

Fig. 5. Effect of δ on the velocity profile.

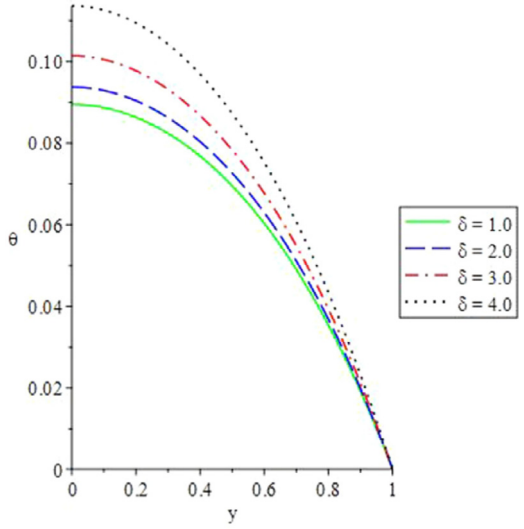

Fig. 6. Heat distribution for rising δ.

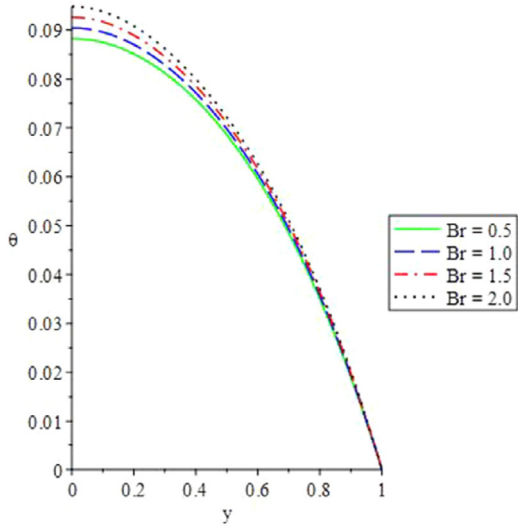

Fig. 7. Temperature field for various *Br*.

4.2. Criticality and explosion slice bifurcation solutions

It is important to obtain the criticality branch bifurcation for an exothermic reaction; this is characterized by the Frank-Kamenenetskii term λ_{cr}. For $\lambda > \lambda_{cr}$, there is an existence of disappearance of steady solution. From the explosion theory, thermal explosion or criticality exists when $d\lambda/d\theta_{max} = 0$ for $\theta_{max} = \theta(0)$. To evaluate critical value λ_{cr}, λ in Eq. (10) is assumed to be an unknown and the equation is treated as an eigenvalue problem. Here, the branching system is solved using weighted residual method. The criticality solution branches in the plane $(\lambda_{cr}, \theta_{max})$ for $0 < \epsilon < < 1$, $n \in \{-2, 0, 1/2\}$ and $m \in \{1, 2, 3, 4\}$ is depicted in the Figs. 8, 9 and 10. These show the qualitative difference in the conducting exothermic reactive fluid temperature θ_{max} with rising in the term λ_{cr}. A unique solution exists when $\lambda_{cr} \to 0$. However, for the various values of terms considered ϵ, n and m, turning point exist with branches of solution that denotes branch-chain thermal criticality λ_{cr} as seen in the plots. The first solutions branch for the parameters variation is either increase or decrease for the heat θ_{max} with less significant as the exothermic reaction increases. However, for each case of the parameters, the second solution branch of the phenomenon behaved opposite to the first solution with high significance. No real solution is obtained when $\lambda_{cr} < \lambda$ but a classical form which connotes thermal explosion. The

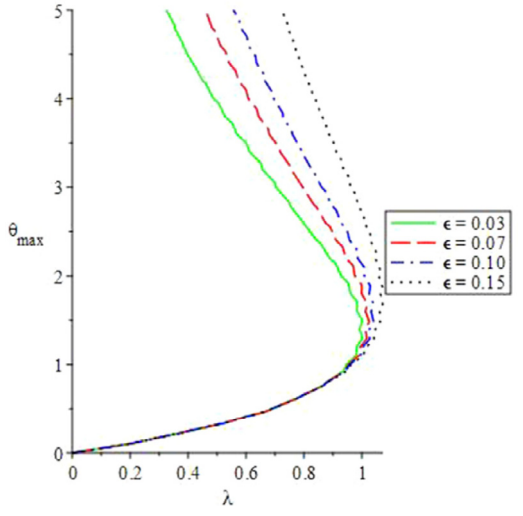

Fig. 8. Criticality branch-chain for rising ϵ.

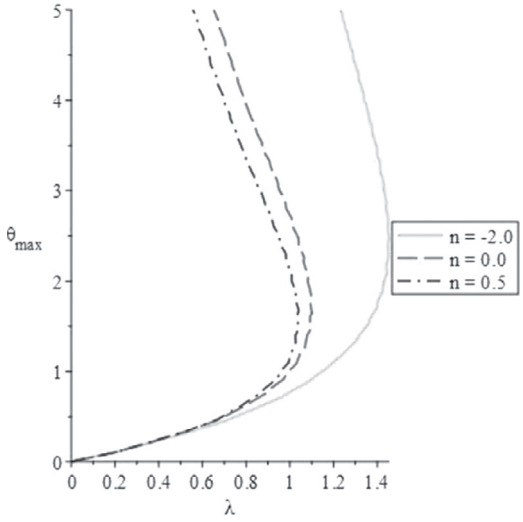

Fig. 9. Branch-chain for various n.

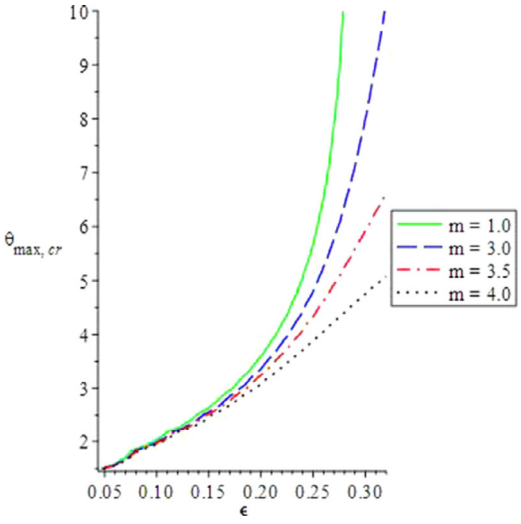

Fig. 11. Plot of $\theta_{max,cr}$ against ϵ for m.

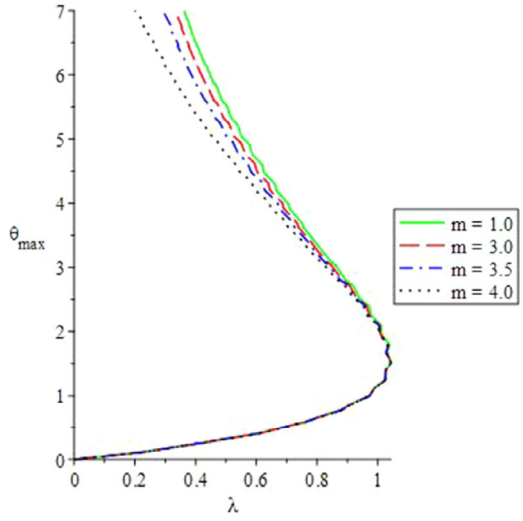

Fig. 10. Bifurcation slice for different m.

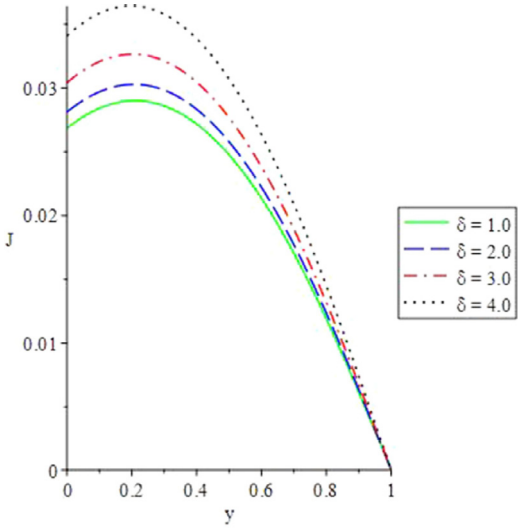

Fig. 12. Current density for increasing δ.

plot of $\theta_{max,cr}$ against ϵ is reported in Fig. 11. A decrease in the exothermic system is gotten on rising in the temperature index m. This shows that the non-Newtonian exothermic reaction can be managed with variation in the heat exponent.

4.3. Current density parameters solutions dependent

The plot of J against y for increasing the values of the terms δ, G, λ and Λ is demonstrated in Figs. 12, 13, 14 and 15. The electric loading field δ, gradient pressure G, Frank-Kamenetskii λ terms increase the electric charge distribution in the combustible second-grade reactive fluid. A rise in the flow of charge carrying particles in the channel space to those atoms or particles which are deficient in electron is noticed as the values of the terms are raised. The magnitude increases because more heat is produced in the system that leads to declination in the fluid viscoelastic bonding force. A discouragement in the liquid bonding force allows free collision of charge carrier particles in space within the Poiseuille device. However, the reverse is the case for the second-grad material term Λ that damped the current density profile. The electrical charge carrying particles could not transmit in space due to an increase in the bonding force of the viscoelastic fluid that barred free particle movement in the channel. This then result to diminish in the current density field.

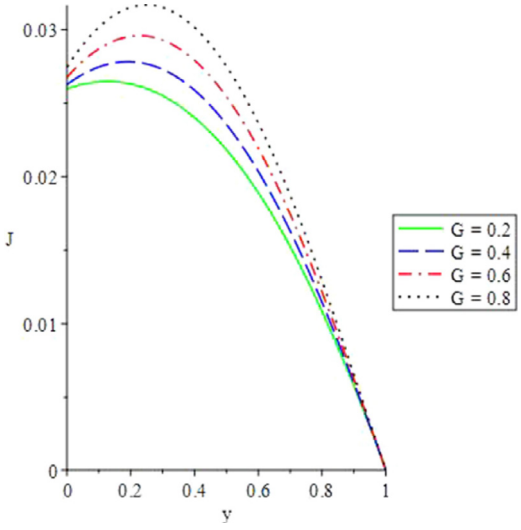

Fig. 13. Current density for rising in G.

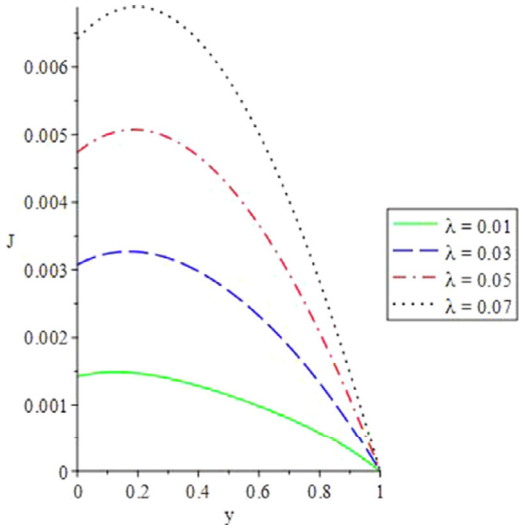

Fig. 14. Effect of λ on current density.

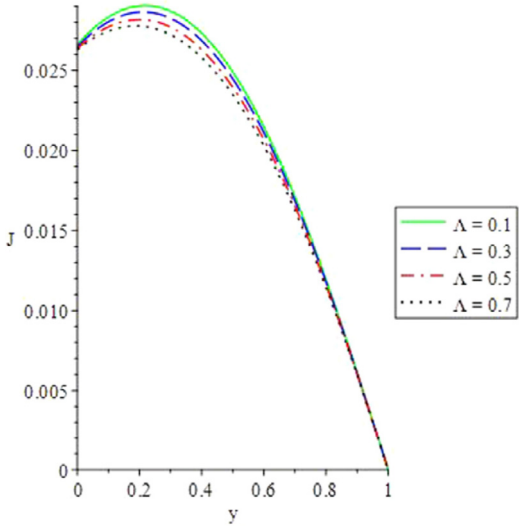

Fig. 15. Impact of Λ on current density.

5. Conclusion

A computational investigation of the current density and criticality for a reactive Poiseuille second-grade flow with variable conductivity via finite difference of semi-discretization method is considered. The electric loading field is noticed to have reduced the flow rate, but enhances the temperature distribution. Nevertheless, its worth mention that parameters that raises the thermal criticality regime must be monitored to circumvent explosion of the reactive solution. The critical region is an area that separates ignition and non-ignition of the combustible reaction. Moreover, terms that increases current density in the flow system need to be augmented to improve the current carrying hydromagnetic fluid for industrial usage. This is necessary in order to enhance lubricants viscosity for the operations of manufacturing and engineering device at optimum performance.

Declaration of Competing Interest

All authors have agreed and approved the manuscript and have contributed significantly towards the article. There is no conflict of interest among the authors.

References

[1] K. Al-Khaled, S.U. Khan, I. Khan, Chemically reactive bioconvection flow of tangent hyperbolic nanoliquid with gyrotactic microorganisms and nonlinear thermal radiation, Heliyon J. 6 (1) (2020) e03117.
[2] S.U. Khan, H. Waqas, M.M. Bhatti, M. Imran, Bioconvection in the rheology of magnetized couple stress nanofluid featuring activation energy and Wu's slip, J. Non-Equilibr. Thermodyn. 45 (1) (2020) 81–95.
[3] S.O. Salawu, H.A. Ogunseye, Entropy generation of a radiative hydromagnetic Powell-Eyring chemical reaction nanofluid with variable conductivity and electric field loading, Results Eng. 5 (2020) 100072.
[4] I. Tlili, H. Waqas, A. Almaneea, S.U. Khan, M. Imran, Activation energy and second order slip in bioconvection of oldroyd-b nanofluid over a stretching cylinder: a proposed mathematical model, Processes 7 (12) (2019) 914.
[5] A. Alwatban, S.U. Khan, H. Waqas, I. Tlili, Interaction of Wu's slip features in bioconvection of eyring powell nanoparticles with activation energy, Processes 7 (11) (2019) 859.
[6] A.R. Hassan, J.A. Gbadeyan, S.O. Salawu, The effects of thermal radiation on a reactive hydromagnetic internal heat generating fluid flow through parallel porous plates, Springer Proc. Math. Stat. 259 (2018) 183–193.
[7] S.O. Salawu, N.K. Oladejo, M.S. Dada, Analysis of viscous dissipative poiseuille fluid flow of two-step exothermic chemical reaction through a porous channel with convective cooling, Ain Shams Eng. J. 10 (2019) 565–572.
[8] S. Yasutomi, S. Bair, W.O. Winer, Application of a free volume model to lubricant rheology: I dependence of viscosity on temperature and pressure, ASME J. Tribol. 106 (2) (1984) 291–303.
[9] W.M. Kays, M.E. Crawford, Convective Heat and Mass Transfer, McGraw-Hill, New York, NY, USA, 1980.
[10] N.S. Kobo, O.D. Makinde, Second law analysis for a variable viscosity reactive Couette flow under arrhenius kinetics, Math. Probl. Eng. 10 (2010) 15.
[11] S.O. Salawu, M.S. Dada, O.J. Fenuga, Thermal explosion and irreversibility of hydromagnetic reactive couple stress fluid with viscous dissipation and Navier slips, Theor. Appl. Mech. Lett. 9 (2019) 246–253.
[12] S.O. Salawu, R.A. Oderinu, A.D. Ohaegbue, Thermal runaway and thermodynamic second law of a reactive couple stress hydromagnetic fluid with variable properties and Navier slips, Sci. Afr. 7 (2020) e00261.
[13] Z. Abbas, T. Hayat, M. Sajid, S. Asghar, Unsteady flow of a second grade fluid film over an unsteady stretching sheet, Math. Comput. Model. 48 (2008) 518–526.
[14] A. Ahmad, S. Afzal, S. Asghar, Semi-inverse solution for transient MHD flow of a second grade fluid past a stretching surface, AIP Adv. 5 (2015) 127140–127147.
[15] S.C. Dileep, V. Kumar, Unsteady flow of a non-newtonian second grade fluid in a channel partially filled by a porous medium, Adv. Appl. Sci. Res. 3 (1) (2012) 75–94.
[16] R.A. Kareem, S.O. Salawu, Y. Yan, Analysis of transient Rivlin-Ericksen fluid and irreversibility of exothermic reactive hydromagnetic variable viscosity, J. Appl. Comput. Mech. 6 (1) (2020) 26–36.
[17] T. Hayat, Z. Abbas, M. Sajid, S. Asghar, The influence of thermal radiation on MHD flow of a second grade fluid, Int. J. Heat Mass Transf. 50 (2007) 931–941.
[18] T. Hayat, Z. Abbas, Heat transfer analysis on the MHD flow of a second grade fluid in a channel with porous medium, Chaos Solit. Fract. 38 (2008) 556–567.
[19] M. VeeraKrishna, G.S. Reddy, Unsteady MHD convective flow of second grade fluid through a porous medium in a rotating parallel plate channel with temperature dependent source, Mater. Sci. Eng. 149 (2016) 012216.
[20] M. Sajid, I. Ahmad, T. Hayat, M. Ayub, Unsteady flow and heat transfer of a second grade fluid over a stretching sheet, Commun. Nonlinear Sci. Numer. Simul. 14 (2009) 96–108.
[21] S. Samiulhaq Ahmad, D. Vieru, I. Khan, S. Shafie, Unsteady magnetohydrodynamic free convection flow of a second grade fluid in a porous medium with ramped wall temperature, PLOS ONE 9 (5) (2014) e88766.
[22] F. Ali, I. Khan, S. Shafie, Closed form solutions for unsteady free convection flow of a second grade fluid over an oscillating vertical plate, PlOS ONE 9 (2) (2014) e85099.
[23] S.O. Salawu, R.A. Kareem, S.A. Shonola, Radiative thermal criticality and entropy generation of hydromagnetic reactive Powell Eyring fluid in saturated porous media with variable conductivity, Energy Rep. 5 (2019) 480–488.
[24] S.S. Okoya, On criticality and disappearance of criticality for a branched-chain thermal reaction with distributed temperature, Afr. Mat. 24 (2013) 465–476.
[25] O.D. Makinde, Thermal ignition in a reactive viscous flow through a channel filled with a porous medium, J. Heat Transf. 128 (2006) 601–604.
[26] O.D. Makinde, Thermal criticality for a reactive gravity driven thin film flow of a third-grade fluid with adiabatic free surface down an inclined plane, Appl. Math. Mech. Engl. Ed. 30 (3) (2009) 373–380.
[27] S.S. Okoya, Disappearance of criticality for reactive third-grade fluid with Reynold's model viscosity in a flat channel, Int. J. Non-Linear Mech. 46 (2011) 1110–1115.
[28] T. Chinyoka, O.D. Makinde, Numerical investigation of entropy generation in unsteady MHD generalized couette flow with variable electrical conductivity, The Scientific World Journal 13 (2013) 11.
[29] R.L. Fosdick, K.R. Rajagopal, Anomalous feature in the model of second-order fluids, Arch. Ratio Mech. Anal 70 (1979) 145–152.
[30] C.A. Truesdell, On the foundations of mechanics of energies, in: C.A. Tuesdell (Ed.), (Continuum Mechanics II: The Rational Mechanics of Materials, Gordon and Beach Press, New York, 1965.
[31] S.O. Salawu, A.R. Hassan, A. Abolarinwa, N.K. Oladejo, Thermal stability and entropy generation of unsteady reactive hydromagnetic Powell-Eyring fluid

with variable electrical and thermal conductivities, Alexandria Eng. J. 58 (2019) 519–529.
[32] L. Rundora, O.D. Makinde, Unsteady MHD flow of non-newtonian fluid in a channel filled with a saturated porous medium with asymmetric Navier slip and convective heating, Appl. Math. Inf. Sci. 12 (3) (2018) 483–493.
[33] O.D. Makinde, T. Chinyoka, Numerical study of unsteady hydromagnetic generalized Couette flow of a reactive third-grade fluid with asymmetric convective cooling, Comput. Math. Appl. 61 (2011) 1167–1179.
[34] T. Chinyoka, Computational dynamics of a thermally decomposable visco-elastic lubricant under shear, Trans. ASME J. Fluids Eng. 130 (12) (2008) 7.121201.